Mossbauer spectroscopy of $NH_4Co_{0.994}Fe_{0.006}Cl_3$ and $CsCo_{0.99}Fe_{0.01}Cl_3$

1995 J. Phys.: Condens. Matter 7 1933

(http://iopscience.iop.org/0953-8984/7/9/017)

J. Phys.: Condens. Matter 7 (1995) 1933–1947. Printed in the UK

Mössbauer spectroscopy of $NH_4Co_{0.994}Fe_{0.006}Cl_3$ and $CsCo_{0.99}Fe_{0.01}Cl_3$

Nicholas I Sheen and Valda H McCann

Department of Physics and Astronomy, University of Canterbury, Private Bag 4800, Christchurch 1, New Zealand

Received 1 November 1994

Abstract. Mössbauer spectra of $NH_4Co_{0.994}Fe_{0.006}Cl_3$ have been recorded in the temperature range 1.3 to 250 K. The spectra are similar to those of isostructural $CsCo_{0.99}Fe_{0.01}Cl_3$ which is a quasi-one-dimensional Ising-like antiferromagnet. For $NH_4Co_{0.994}Fe_{0.006}Cl_3$ the transition to a partially disordered magnetic state occurs at $T_{N_1} = (27 \pm 2)$ K and to the fully magnetically ordered state at $T_{N_2} = (11 \pm 2)$ K. As for $CsCo_{0.99}Fe_{0.01}Cl_3$ the relaxation processes evident in the spectra were analysed using the stochastic model of Blume and Tjon with electronic relaxation occurring for Fe^{2+} in the three-dimensionally ordered chains below T_{N_1} and magnetic field reversal, attributed to solitons, in the one-dimensionally ordered chains in the partially disordered phase. Models developed for $CsCo_{0.99}Fe_{0.01}Cl_3$ were extended to include relaxation involving all the Fe^{2+} occupied electronic levels below T_{N_1} (i.e. the three lowest levels) and to allow both electronic and soliton relaxation to occur in the one-dimensionally ordered chains. The data for $NH_4Co_{0.994}Fe_{0.006}Cl_3$ and previous data for $CsCo_{0.99}Fe_{0.01}Cl_3$ were both analysed with these extended models. Relaxation rates were lower than those predicted theoretically for pure $CsCoCl_3$. This may be due to the presence of iron in the cobalt chains changing the soliton dynamics.

1. Introduction

$CsCoCl_3$ is a good example of a quasi-one-dimensional, Ising-like antiferromagnet, of interest because of the prediction by Villain in 1975 of moving domain walls (or solitons) in such antiferromagnets. In these compounds a soliton is a one lattice unit wide domain wall between the two different antiferromagnetically ordered configurations. Using electron spin resonance Adachi (1981) first confirmed the presence of solitons in $CsCoCl_3$. More quantitative work was done (Boucher *et al* 1985) using inelastic neutron scattering.

The one-dimensional nature of $CsCoCl_3$ arises from its perovskite crystal structure: chains of trigonally distorted $CoCl_6$ octahedra are arranged in a triangular lattice, separated by large Cs^+ ions. The space group is $P6_3/mmc$, with lattice parameters $a = (7.2019 \pm 0.0004)$ Å and $c = (6.0315 \pm 0.0005)$ Å (Soling 1968). At 25 °C NH_4CoCl_3 has the same space group as $CsCoCl_3$, with lattice parameters $a = (6.967 \pm 0.001)$ Å and $c = (6.010 \pm 0.001)$ Å (Swanson *et al* 1968). Due to the similar crystal structures and bond angles within the chains of Co^{2+} ions, NH_4CoCl_3 and $CsCoCl_3$ are expected to have similar exchange interactions and magnetic phases, with the smaller lattice parameters of NH_4CoCl_3 resulting in slightly stronger exchange interactions.

The two main exchange interactions between Co^{2+} ions in $CsCoCl_3$ are the antiferromagnetic superexchange between nearest Co^{2+} neighbours within a chain, with exchange constant J, and the antiferromagnetic superexchange between Co^{2+} ions on

0953-8984/95/091933+15$19.50

neighbouring chains, with exchange constant J'. Various experiments (Shiba 1980, Nagler *et al* 1983, Ohta *et al* 1993) confirm the one-dimensional nature of $CsCoCl_3$, with J'/J in the range 0.006 to 0.022.

In paramagnetic $CsCoCl_3$ the ground state of the Co^{2+} ions in the trigonally distorted cubic crystal field is a Kramers doublet (Euler and Garrett 1981). Within the chains, the nearest-neighbour Co^{2+} spins interact according to the effective $S = \frac{1}{2}$ Hamiltonian

$$\mathcal{H} = 2J \sum_i [S_i^z S_{i+1}^z + \varepsilon(S_i^x S_{i+1}^x + S_i^y S_{i+1}^y)] \tag{1}$$

where the sum is over the spins i within the chain. J and ε have been determined to be 75 K and 0.12 respectively (Achiwa 1969, Tellenbach 1978, Yoshizawa *et al* 1981). The positive sign of J in this Hamiltonian signifies that the intrachain exchange interaction is antiferromagnetic. The low value of ε means that the Hamiltonian is Ising-like, and so has soliton solutions as shown by Villain (1975).

Due to the large ratio of the intra to interchain exchange interactions, short-range antiferromagnetic order along the chains of Co^{2+} spins develops before the onset of three-dimensional ordering. In $CsCoCl_3$ the transition from paramagnetism to short-range order occurs at $\approx$75 K (Boucher *et al* 1985). Below 75 K the intrachain correlation length gradually increases until the transition to the partially disordered phase at T_{N_1} is reached. Three measurements (Melamud *et al* 1974, Mekata and Adachi 1978, Yoshizawa and Hirakawa 1979) of the first Néel temperature can be combined to give $T_{N_1} = 21.2$ K.

Co^{2+} ions are arranged in a triangular lattice within the a–b plane so below T_{N_1} a partially disordered phase occurs with two thirds of the chains correlated and one third of the chains frustrated and showing only one-dimensional magnetic order. From the work of Villain solitons are expected in the frustrated chains.

At temperatures below $T_{N_2} \simeq$ 8–9 K (Mekata and Adachi 1978, Yoshizawa and Hirakawa 1979) the second nearest-neighbour interchain exchange interaction is important in $CsCoCl_3$, and full three-dimensional ferrimagnetic ordering occurs. In this phase all spins in the frustrated chains are ferromagnetically correlated with the second-nearest interchain neighbours (the nearest frustrated chains).

The magnetic phases of NH_4CoCl_3 are expected to be similar to those of $CsCoCl_3$, with slightly higher ordering temperatures, consistent with stronger exchange interactions in the NH_4CoCl_3 salt. T_{N_1} has been found approximately from the Mössbauer spectra taken by Asch *et al* (1973) to be (27 ± 4) K.

$CsCoCl_3$ and NH_4CoCl_3 were doped with ^{57}Fe, enabling Mössbauer spectra to be taken. The Fe^{2+} ions were expected to randomly replace the Co^{2+} ions and participate in the magnetic ordering.

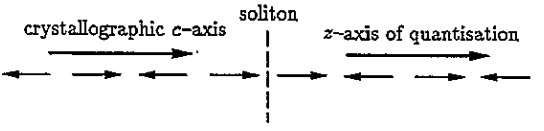

Figure 1. A chain of Co^{2+} spins in $CsCoCl_3$ or NH_4CoCl_3.

Within the effective $S = \frac{1}{2}$ Hamiltonian (equation (1)) a soliton can be thought of in a semiclassical model as 'flipping the spin' of successive spins along the chain of Co^{2+} ions. This is illustrated in figure 1. After the passage of a soliton, a spin in the chain experiences an intrachain exchange with its neighbours which is exactly the same as if the direction of the z axis had been reversed. Due to energy considerations the Co^{2+} ion must be in the

ground state in this new environment, and so the signs of the z components of $\boldsymbol{L}$ and $\boldsymbol{S}$ are reversed. Hence the only effect on the Co^{2+} ion of the passage of a soliton is an effective reversal of the z axis of quantisation, and the soliton is a 'topological' excitation. By the same reasoning, the sign of the magnetic hyperfine field (B_{hf}) at the Fe^{2+} ion, which is proportional to L_z and S_z, is reversed on the passage of a soliton.

B_{hf} is also changed when relaxation occurs between the electronic states of the Fe^{2+} ion. In their study of the Mössbauer spectra of $CsCoCl_3$ Ward *et al* (1987) observed slow (0.5 to 40 MHz) paramagnetic relaxation between the lowest two electronic states of Fe^{2+} in the ordered sites at temperatures between T_{N_2} and T_{N_1}, and in all sites at temperatures below T_{N_2}. This relaxation was reported to be thermally activated with an activation energy of (42 ± 8) K, much lower than the activation energy of 75 K reported for solitons in pure $CsCoCl_3$ by Boucher *et al* (1985). It appears that the 'electronic' relaxation in the Fe^{2+} ion dopant is similar to that of a paramagnetic ion in a magnetically dilute crystal, caused by interactions between the ion and the phonon bath. It is unusual to observe slow paramagnetic relaxation in the Mössbauer spectra of a magnetically ordered crystal. This unusual relaxation is presumably associated with the intrachain Fe–Co exchange interaction being weaker than the interaction of one chain of Co^{2+} spins with its neighbours. In this case three-dimensional order may occur between chains while the Fe^{2+} ion exhibits relaxation, as observed in the Mössbauer spectra taken by Ward *et al* (1987). Similar electronic relaxation is expected in $NH_4Co_{0.994}Fe_{0.006}Cl_3$.

Ward *et al* (1987) developed the two-level relaxation model, based on the stochastic model of Blume and Tjon (1968), for their analysis of the Mössbauer spectra of $CsCo_{0.99}Fe_{0.01}Cl_3$. In this model it was assumed that only the two lowest electronic states of Fe^{2+} were occupied significantly, and that in the chains of frustrated spins the Mössbauer spectrum was dominated by soliton relaxation. The soliton relaxation rate that they obtained was much lower than expected from the results of inelastic neutron scattering experiments on $CsCoCl_3$ (Boucher *et al* 1985). Also, some of the results they obtained were not consistent with the model, namely:

(i) The soliton relaxation rate in the frustrated chains was not significantly faster than the Fe^{2+} electronic relaxation rate obtained from the subspectrum corresponding to the three-dimensionally ordered chains. This is contrary to the assumption of the model that in the chains of frustrated spins the relaxation is dominated by solitons.

(ii) From fits to the Mössbauer spectra taken below T_{N_1}, the magnetic hyperfine field B_{hf} decreased with increasing temperature, in contrast with the prediction that the B_{hf} associated with the lowest magnetic state of Fe^{2+} should be independent of temperature.

(iii) According to preliminary calculations, the electronic energy levels of the Fe^{2+} ion in $CsCo_{0.99}Fe_{0.01}Cl_3$ are such that a third electronic state is significantly populated at temperatures above about 15 K.

The departure from the two-level relaxation model due to thermal occupation of the third electronic state of Fe^{2+} was expected to be greater in $NH_4Co_{0.994}Fe_{0.006}Cl_3$, which has a higher T_{N_1}. In order to account for the occupation of the third electronic state the three-level relaxation model was developed. In the three-level relaxation model the electronic relaxation evident in the Mössbauer spectra was assumed to occur by the direct relaxation process, as for paramagnetic relaxation.

A further refinement is that of the combined relaxation model which was developed to calculate Mössbauer lineshapes when two different relaxation processes occur at the same site. This situation arises at $^{57}Fe^{2+}$ ions in the frustrated chains of $CsCo_{0.99}Fe_{0.01}Cl_3$ and $NH_4Co_{0.994}Fe_{0.006}Cl_3$, where both soliton and electronic relaxation occur. These models of

the relaxation processes are described in section 2.2. Experimental details in section 3 are followed by results and analysis of the Mössbauer spectra in terms of the relaxation models in section 4. Conclusions are drawn in section 5.

2. Theory

2.1. Determination of Fe^{2+} electronic Hamiltonian parameters

The Fe^{2+} ions substitute for the Co^{2+} ions into sites with point symmetries of $\bar{3}m$ and $3m$ for $CsCoCl_3$ and NH_4CoCl_3 respectively. In the case of these Ising-like systems, where the magnetic exchange field (which is parallel to B_{hf}) is along the crystallographic c axis, the electronic Hamiltonian for Fe^{2+} is (Sugano *et al* 1970 p 134, Ballhausen 1962)

$$\begin{aligned}\mathcal{H} &= \mathcal{H}_{\text{octahedral}} + \mathcal{H}_{\text{trigonal}} + \mathcal{H}_{\text{spin-orbit}} + \mathcal{H}_{\text{exchange}} \\ &= B_C^4[C_0^{(4)} + (\tfrac{10}{7})^{1/2}(C_3^{(4)} - C_{-3}^{(4)})] + (B_0^2 C_0^{(2)} + B_0^4 C_0^{(4)}) \\ &\quad + \lambda \boldsymbol{L}\cdot\boldsymbol{S} - J_{\text{eff}}\langle S_{\text{Co}}\rangle S_z. \end{aligned} \tag{2}$$

Here B_C^4 is the cubic crystal field parameter, and B_0^2 and B_0^4 are the trigonal and second-order axial crystal field parameters respectively. The normalised spherical harmonic operators are defined by Sugano *et al* (1970 p 7) as $C_m^{(k)}(\theta,\phi) = [4k/(2k+1)]^{1/2} Y_{km}(\theta,\phi)$. The Y_{km} are the usual spherical harmonics, λ is the spin–orbit parameter, J_{eff} is the effective exchange constant, and S_z is the z component of the spin S of the Fe^{2+} ion. The thermal average of the host Co^{2+} spin is $\langle S_{\text{Co}}\rangle$, given by the $S = \frac{1}{2}$ Brillouin function (Kittel 1976).

The crystal field and spin–orbit parameters were obtained by diagonalizing the electronic Hamiltonian in the basis of the 25 Fe^{2+} 3d states (Ward *et al* 1987), and fitting the quadrupole splitting, QS, at temperatures above T_{N_1} (where $\langle S_{\text{Co}}\rangle = 0$). The QS of each eigenstate of the electronic Hamiltonian is given by $\text{QS} = \frac{1}{2}|e|QV_{zz}$ where

$$V_{zz} = V_{zz}^{\text{val}} + V_{zz}^{\text{lat}}. \tag{3}$$

$$V_{zz}^{\text{val}} = \frac{1}{42\pi\varepsilon_0}|e|\langle r_Q^{-3}\rangle\left\{3L_z^2 - L(L+1)\right\}$$

where the expectation value $\langle O\rangle$ of an operator O refers to a particular eigenstate of Fe^{2+} and V_{zz}^{lat} is the contribution to V_{zz} from the rest of the crystal. The QS above T_{N_1} is then found by taking the average of V_{zz} over the thermally populated eigenstates of the Fe^{2+} electronic Hamiltonian.

The magnetic hyperfine field B_{hf} for each eigenstate of the electronic Hamiltonian can be calculated from the sum of the Fermi contact, orbital, and dipolar contributions (Ingalls 1971),

$$\begin{aligned}\boldsymbol{B}_{\text{hf}} &= \tfrac{1}{2}B_c\langle\boldsymbol{S}\rangle + (\mu_0\mu_B/2\pi)\langle r^{-3}\rangle\langle\boldsymbol{L}\rangle \\ &\quad + (\mu_0\mu_B/84\pi)\langle r^{-3}\rangle\langle\left[\tfrac{3}{2}[\boldsymbol{L}(\boldsymbol{L}\cdot\boldsymbol{S}) + (\boldsymbol{L}\cdot\boldsymbol{S})\boldsymbol{L}] - L(L+1)\boldsymbol{S}\right]\rangle. \end{aligned} \tag{4}$$

For Fe^{2+} in $NH_4Co_{0.994}Fe_{0.006}Cl_3$ and $CsCo_{0.99}Fe_{0.01}Cl_3$ above T_{N_1} the low-lying eigenstates of the electronic Hamiltonian are a ground eigenstate, which produces no magnetic hyperfine field, and a magnetic doublet 10 to 15 cm^{-1} above. At temperatures below T_{N_1} the doublet is split by the magnetic exchange interaction with the Co^{2+}neighbours. At 2.8 K the relaxation rate is sufficiently slow for accurate determination from the magnetic subspectrum of the magnetic hyperfine field B produced by the magnetic substate. As $\langle r^{-3}\rangle$ and B_c cannot be found independently, $\langle r^{-3}\rangle$ was fixed at a physically reasonable value (4.0 au) and B_c was then determined from this measured value of the magnetic hyperfine field.

2.2. Relaxation models

In the two-level relaxation model the nuclear Hamiltonian is

$$\mathcal{H}(t) = \mathcal{H}_0 + Q'(3I_z^2 - I^2) + g\mu B I_z f(t). \tag{5}$$

$\mathcal{H}_0$ is the unperturbed Hamiltonian for the nucleus in the absence of fields and Q' is the nuclear quadrupole moment operator. The unperturbed Hamiltonian has the property

$$\mathcal{H}_0|I_0m_0\rangle = E_0|I_0m_0\rangle \qquad \mathcal{H}_0|I_1m_1\rangle = E_1|I_1m_1\rangle.$$

The g factors for the ground and excited states are given by

$$g|I_0m_0\rangle = g_0|I_0m_0\rangle \qquad g|I_1m_1\rangle = g_1|I_1m_1\rangle$$

and

$$Q'|I_0m_0\rangle = 0 \qquad Q'|I_1m_1\rangle = \frac{|e|QV_{zz}}{4I_1(2I_1-1)}|I_1m_1\rangle.$$

$f(t)B$ is the instantaneous value of the magnetic hyperfine field, and $f(t)$ is a stochastic random function of time. If $f(t)$ assumes values of unity and zero then equation (5) models electronic relaxation between the two lowest-energy eigenstates, producing magnetic hyperfine fields of B and 0. If $f(t)$ assumes values of 1 and -1, equation (5) models the situation where soliton relaxation dominates electronic relaxation and the magnetic hyperfine field reverses.

Following Abragam (1961) it is assumed that $f(t)$ is a stationary Markov function, and the function $W(f_2|f_1, \Delta t)$ is defined as the probability that $f(t + \Delta t) = f_2$ given that $f(t) = f_1$. When Δt is small enough, $W(f_2|f_1, \Delta t)$ can be expanded in a power series of Δt, and when higher orders of Δt are discarded, for $f_2 \neq f_1$

$$W(f_2|f_1, \Delta t) \simeq \pi(f_1, f_2)\Delta t \tag{6}$$

since $W(f_2|f_1, 0) = 0$ when $f_2 \neq f_1$. From the definition of equation (6),

$$\pi(f_1, f_2) = \frac{\mathrm{d}}{\mathrm{d}\,\Delta t} W(f_2|f_1, \Delta t)\bigg|_{\Delta t=0}. \tag{7}$$

For the case $f_2 = f_1$,

$$W(f_1|f_1, \Delta t) \simeq 1 + \pi(f_1, f_1)\Delta t \tag{8}$$

since $W(f_1|f_1, 0) = 1$. The sum of the probabilities W must equal unity, that is $\sum_{f_2} W(f_2|f_1, \Delta t) = 1$, so consequently

$$\pi(f_1, f_1) = -\sum_{f_2 \neq f_1} \pi(f_1, f_2). \tag{9}$$

In units of $\hbar = 1$, the Mössbauer lineshape as a function of frequency ω is (Blume and Tjon 1968, Abragam 1961)

$$I(\omega) = \mathrm{Re} \sum_{m_0 m_1} D_{m_0 m_1} K \cdot A^{-1} \cdot \mathbf{1} \tag{10}$$

where $D_{m_0m_1} \equiv (1/\Gamma)\left|\langle I_1 m_1|\mathcal{H}^-|I_0 m_0\rangle\right|^2$, and K_μ is the diagonal matrix formed from the occupation probabilities for the different values of $f(t)$. Also, $A_{\mu\nu} \equiv \mathrm{i}(\alpha F_{\mu\nu} - \mathcal{E}\delta_{\mu\nu}) + \pi_{\mu\nu} - (\Gamma/2)\delta_{\mu\nu}$, where $\alpha \equiv (g_0m_0 - g_1m_1)\mu B$, $F_{\mu\nu} \equiv f_\mu\delta_{\mu\nu}$ is a diagonal matrix of the values of the stochastic function $f(t)$, and $\mathcal{E} \equiv -(\omega - \omega_0 - \frac{1}{12}|e|QV_{zz}(3m_1^2 - \frac{15}{4}))$ with $\omega_0 = E_1 - E_0$. Γ is the experimentally observed full width at half maximum depth of the absorption line (found from spectra taken at temperatures above those affected by short-range magnetic ordering), and $\pi_{\mu\nu} \equiv \pi(f_\mu, f_\nu)$ is the relaxation matrix.

In the three-level relaxation model, $f(t)$ in equation (5) assumes values of 1, 0 and -1 for sites in the three-dimensionally ordered chains, and ± 1 for the sites in the frustrated chains. For sites in the frustrated chains the 3×3 relaxation matrix π has three independent elements. To avoid undetermined parameters it was necessary to assume that the electronic relaxation occurs by some spin–phonon relaxation mechanism, as for a paramagnetic centre. The Raman process was rejected because the relaxation rates obtained by fits using the two-level relaxation model to $NH_4Co_{0.994}Fe_{0.006}Cl_3$ and $CsCo_{0.99}Fe_{0.01}Cl_3$ spectra (shown in figures 4 and 7) did not show the T^7 dependence on temperature characteristic of the Raman process for non-Kramers ions (Abragam and Bleaney 1970 p 563). The electronic relaxation was assumed to occur by the direct process. For transitions from a lower-energy state $|\psi_i\rangle$ to a higher-energy state $|\psi_j\rangle$, separated by energy E, the rate $\pi_f\uparrow$ given that the initial state is occupied is (Abragam and Bleaney 1970 p 558)

$$\pi_f\uparrow = \omega_0 \frac{E^3}{\exp[E/(kT)] - 1} \tag{11}$$

where ω_0 is a parameter that is fitted, and in the simplest approximation is related to the density ρ, the speed of sound in the crystal v, and the matrix element of the term linear in strain, $V^{(1)}$, in the expansion of the crystalline electric potential $V = V_0 + \epsilon V^{(1)} + \epsilon^2 V^{(2)} + \cdots$,

$$\omega_0 = \frac{3|\langle\psi_j|V^{(1)}|\psi_i\rangle|^2}{2\pi\hbar^4\rho v^5}. \tag{12}$$

The rate $\pi_f\downarrow$ for transitions from a higher-energy state to a lower-energy state is

$$\pi_f\downarrow = \omega_0 \frac{E^3 \exp[E/(kT)]}{\exp[E/(kT)] - 1}. \tag{13}$$

Equations (11) and (13) are used for the off-diagonal elements of π, and equation (9) gives the diagonal elements.

In the combined relaxation model the relaxation at sites in the three-dimensionally ordered chains was assumed to be three-level electronic relaxation, as for the three-level relaxation model. In sites in the frustrated chains, both electronic and soliton relaxation processes were assumed to occur independently. This situation can be modelled by the nuclear Hamiltonian

$$\mathcal{H}(t) = \mathcal{H}_0 + Q'(3I_z^2 - I^2) + g\mu B I_z f(t) s(t) \tag{14}$$

where $f(t)$ represents electronic relaxation, and the stochastic function $s(t) = \pm 1$ represents soliton relaxation. The product $f(t)s(t)$ models the situation where solitons flip the sign of the magnetic hyperfine field when $f(t) = \pm 1$, and have no effect when $f(t) = 0$.

Defining $W(f_2 s_2 | f_1 s_1, \Delta t)$ as the probability that $f(t + \Delta t) = f_2$ *and* $s(t + \Delta t) = s_2$ given that $f(t) = f_1$ *and* $s(t) = s_1$, the combined relaxation matrix is obtained by expanding $W(f_2 s_2 | f_1 s_1, \Delta t)$ in a power series in Δt,

$$W(f_2 s_2 | f_1 s_1, \Delta t) \simeq \delta_{f_1, f_2}\delta_{s_1, s_2} + \pi(f_1 s_1, f_2 s_2)\Delta t \tag{15}$$

where π has 36 elements, one for each combination of $f_1, s_1, f_2,$ and s_2.

Assuming that both relaxation processes occur independently, the elements of the combined relaxation matrix π_{fs} can be related to elements of the electronic π_f and soliton π_s relaxation matrices.

$$W_{fs}(yv|xu, \Delta t) = W_f(y|x, \Delta t) W_s(v|u, \Delta t) \tag{16}$$

for $y \neq x$ and $v \neq u$, where x and y label values of $f(t)$, and u and v label values of $s(t)$. $W_s(v|u, \Delta t)$ is the probability that $s(t + \Delta t) = s_v$ given that $s(t) = s_u$.

If both electronic and soliton relaxation have occurred during time Δt, then $y \neq x$ and $v \neq u$, and, using equations (6), (7), and (16),

$$\begin{aligned}\pi_{fs}(xu, yv) &= \frac{\mathrm{d}}{\mathrm{d}\,\Delta t} W_{fs}(yv|xu, \Delta t)\Big|_{\Delta t=0} \\ &= \frac{\mathrm{d}}{\mathrm{d}\,\Delta t}[W_f(y|x, \Delta t) W_s(v|u, \Delta t)]\Big|_{\Delta t=0} \\ &= [\pi_f(x, y) W_s(v|u, \Delta t) + W_f(y|x, \Delta t)\pi_s(u, v)]\big|_{\Delta t=0} \\ &= 2\pi_f(x, y)\pi_s(u, v)\Delta t\big|_{\Delta t=0} = 0.\end{aligned}$$

If, during time Δt, only electronic relaxation has occurred, then $y \neq x$, $v = u$, and

$$\begin{aligned}\pi_{fs}(xu, yu) &= \frac{\mathrm{d}}{\mathrm{d}\,\Delta t}[W_f(y|x, \Delta t) W_s(u|u, \Delta t)]\Big|_{\Delta t=0} \\ &= [\pi_f(x, y)\,(1 + \pi_s(u, u)\Delta t) + \pi_f(x, y)\Delta t\,\pi_s(u, u)]\big|_{\Delta t=0} = \pi_f(x, y).\end{aligned}$$

Likewise, if only soliton relaxation has occurred, $y = x$, $v \neq u$, and $\pi_{fs}(xv, xu) = \pi_s(u, v)$. The diagonal elements of π_{fs} are

$$\pi_{fs}(xu, xu) = -\sum_{yv \neq xu} \pi_{fs}(xu, yv). \tag{17}$$

3. Experimental details

NH_4CoCl_3 doped with nominally 0.5 atomic % ^{57}Fe was grown from a mixture of NH_4Cl and (99.5% $CoCl_2$ + 0.5% $^{57}FeCl_2$). The $CoCl_2/FeCl_2$ mixture was prepared by dissolving ^{57}Fe in dilute aqueous HCl, adding $CoCl_2$, and drying the solution. A small excess of NH_4Cl calculated from the estimated vapour pressure of NH_4Cl at 460 °C (25.4 atm) was added so that the stoichiometric amount of NH_4Cl was present in the melt. The mixture was sealed in an evacuated silica tube, and the crystal was grown by the Bridgman technique.

The standard transmission Mössbauer spectrometer, velocity calibration method, and preparation technique for the polycrystalline absorbers were as discussed in Sheen *et al* (1994).

Chemical analysis of the absorber was performed using a Varian 175 AA atomic absorption spectrometer. It was found that the $NH_4Co_{1-x}Fe_xCl_3$ crystal had a composition of $x = (0.595 \pm 0.002)$ at.% Fe.

4. Results

4.1. Mössbauer spectra of paramagnetic $NH_4Co_{0.994}Fe_{0.006}Cl_3$

At temperatures in the range 27.5 K to 250 K, the spectra show a pair of quadrupole split absorption lines of unequal intensity, as for $CsCo_{0.99}Fe_{0.01}Cl_3$ (Ward *et al* 1987). The cause of the unequal intensity is presumed to be the same as for $CsCo_{0.99}Fe_{0.01}Cl_3$, with the crystallites in the polycrystalline absorber aligning preferentially in the plane of the absorber. The higher-energy line is the most intense, giving $V_{zz} < 0$ consistent with the Mössbauer spectra taken below T_{N_1}. To correct for this effect on the intensities below T_{N_1} the magnetically split $m_I = \pm\frac{1}{2} \rightarrow \pm\frac{3}{2}$ transition absorption lines were multiplied by an empirical correction factor derived from the ratio of the line intensities of the spectra taken above T_{N_1}.

Below 40 K there is a gradual increase of linewidth as the temperature decreases, consistent with magnetic correlations along the c axis (obtained by Ajiro *et al* in 1989).

The QS values above 30 K were fitted using the same general procedure as for $CsCo_{0.99}Fe_{0.01}Cl_3$ (Ward *et al* 1987). With the cubic crystal field parameter fixed to 10 150 cm^{-1}, as for $CsCo_{0.99}Fe_{0.01}Cl_3$, it was found that a very good fit could be obtained for any value of $\langle r_Q^{-3}\rangle$ in the range 3.5 to 4.5 au, if $|B_0^2|$, $|B_0^4|$, and $|\lambda|$ were allowed to become very large. For reasonable values of λ (less than 90% of its free ion value of -104 cm^{-1} (Trees 1951)), and B_0^4 fixed to values less than 3000 cm^{-1}, the energy splittings between the singlet ground state and the first excited doublet were found to be in the range 6.5 to 17 cm^{-1} at 27 K (T_{N_1}). A value of $B_0^4 = 1000$ cm^{-1} was chosen, which gave the greatest stability of χ^2 to variation of $\langle r_Q^{-3}\rangle$, and gave a singlet–doublet splitting at 27 K of ~ 11.3 cm^{-1} for values of $\langle r_Q^{-3}\rangle$ of both 3.5 and 4.5 au. The fits obtained when $\langle r_Q^{-3}\rangle$ was fixed to 3.5 and 4.5 au are shown in figure 2, while the parameters obtained are shown in table 1.

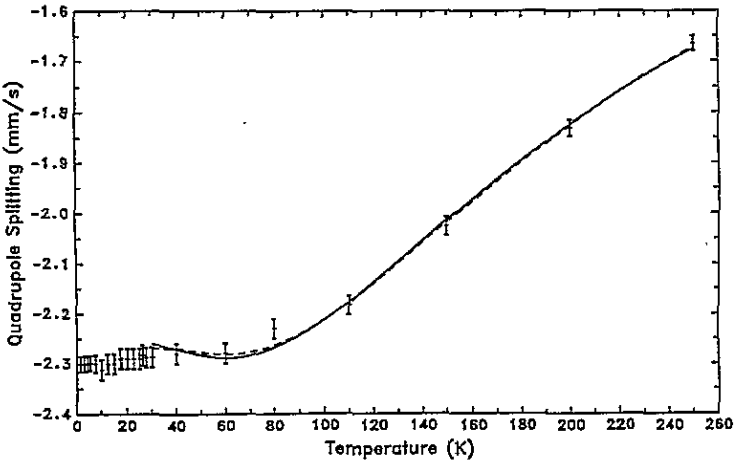

Figure 2. The quadrupole splitting for $NH_4Co_{0.994}Fe_{0.006}Cl_3$ fitted at temperatures above 30 K. The fitted curves were calculated from the eigenstates of the electronic Hamiltonian according to the expectation value of V_{zz} for the different parameter sets in table 1. The dashed (solid) curve corresponds to the parameter set of table 1 with $\langle r_Q^{-3}\rangle$ fixed to 4.5 (3.5) au. The QS at temperatures below 27.5 K is from spectra of $NH_4Co_{0.994}Fe_{0.006}Cl_3$ fitted using the combined relaxation model as described in the theory section.

Table 1. Parameters obtained from fitting the quadrupole splitting data shown in figure 2 using Hamiltonian (2) and QS calculated using equation (3). The superscript f denotes parameters which were fixed during the fit, and the numbers in brackets indicate the uncertainty in the least significant figure(s).

χ^2	$\langle r_Q^{-3}\rangle$ (au)	B_C^4 (cm^{-1})	B_0^2 (cm^{-1})	B_0^4 (cm^{-1})	λ (cm^{-1})	$\frac{1}{2}\lvert e\rvert Q V_{zz}^{lat}$ (mm s^{-1})
1.45	3.5^f	10 150^f	990(20)	1000^f	−64(3)	−0.75(8)
0.92	4.5^f	10 150^f	950(20)	1000^f	−70(3)	−0.65(8)

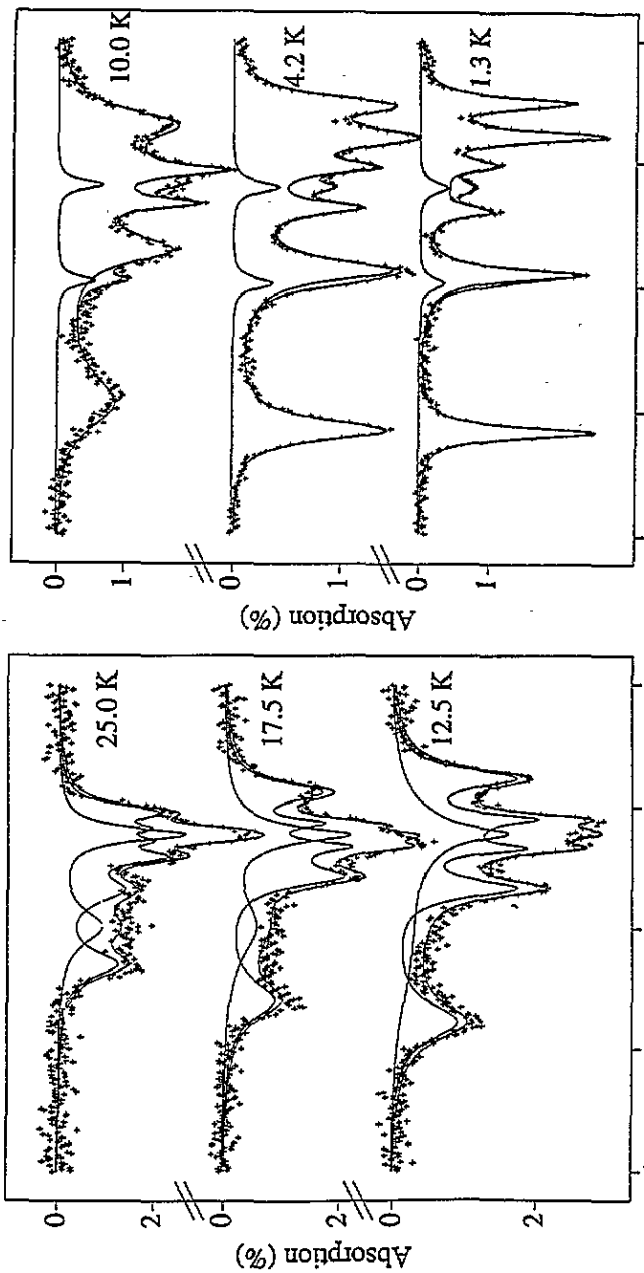

Figure 3. Representative Mössbauer spectra of $NH_4Co_{0.994}Fe_{0.006}Cl_3$ taken at temperatures of 25 K and below. For spectra below 10.0 K the weak quadrupole-split subspectrum has a relative area of 5.5%. The main subspectrum was fitted using the three-level relaxation model. For the spectra taken at temperatures of 12.5 K and above, the fitted curves were obtained using the combined relaxation model. That is, each has a soliton subspectrum *(relative area fixed to* $\frac{1}{3}$*) with the other subspectrum fitted using three-level electronic relaxation only.*

4.2. Mössbauer spectra of magnetically ordered $NH_4Co_{0.994}Fe_{0.006}Cl_3$

Representative Mössbauer spectra of $NH_4Co_{0.994}Fe_{0.006}Cl_3$ taken below T_{N_1} are shown in figure 3. The spectra have unequal broadening of the absorption lines, characteristic of the effect of relaxation processes. The spectra are similar to those of $CsCo_{0.99}Fe_{0.01}Cl_3$ (Ward *et al* 1987) so initially a similar fitting procedure was followed.

At 1.3 K and 2.8 K the spectra are only slightly broadened and can be considered a superposition of two subspectra: one a six-line spectrum with $B_{hf} \sim 22$ T, QS ~ -2.3 mm s^{-1}, isomer shift (IS) ~ 1.23 mm s^{-1}, η (asymmetry parameter) and θ (angle between B_{hf} and the principal z axis of the EFG tensor) both zero; the other a pair of lines with the same QS and IS but with $B_{hf} \sim 0$. This is consistent with having Fe^{2+} in the two lowest electronic states and slow relaxation occurring between these states.

Thus the spectra below 10 K were fitted allowing electronic relaxation between the lowest two states (giving $B_{hf} = B$ and 0). The program also determines the splitting, E_2, between these two states. The spectra could be fitted satisfactorily only if we included an 'extra' pair of lines with a relative area of 5.5% as shown in figure 3. To test whether this was due to the prescence of Fe^{2+} rather than Co^{2+} nearest neighbours in the chain a sample was prepared with a greater (0.84%) concentration of ^{57}Fe. The relative area of the 'extra' lines was greater for this sample so presumably this assumption is correct. However for neither sample could the 'extra' lines be observed at temperatures above T_{N_2} so the origin of these lines remains in doubt.

Assuming that the crystal field parameters and other parameters in the Hamiltonian (equation (2)) are independent of temperature, the remaining parameters to be determined from the low-temperature spectra are the Fermi contact effective field B_c and the effective Fe–Co exchange parameter J_{eff}. These were chosen to give the observed values of B and the splitting, E_2, between the two lowest electronic states for the Mössbauer spectrum at 2.8 K. These values of J_{eff} and B_c are shown in table 2.

Table 2. Values of the parameters J_{eff} and B_c giving the electron state splitting, E_2, and the magnetic hyperfine field, B, found from fitting the spectrum of $NH_4Co_{0.994}Fe_{0.006}Cl_3$ at 2.8 K. The other parameters in the Hamiltonian are given in table 1. The calculated values of E_2 and B for two different values of $\langle r_Q^{-3} \rangle$ are also shown.

$\langle r_Q^{-3} \rangle$ (au)	J_{eff} (cm^{-1})	E_2 (cm^{-1})	B_c (T)	B (T)
4.5	−25	4.2	−55	22.3
3.5	−26	4.2	−53	22.6

Using the wavefunctions of the electronic Hamiltonian, and these values of J_{eff} and B_c, the energy splittings and B_{hf} produced by the three lowest eigenstates were then calculated. It was found that to a good approximation the magnetic hyperfine fields produced by the three lowest eigenstates are parallel to the crystallographic c axis with B (state (1)), 0 T (state (2)), and $-B$ (state (3)). The states are labelled according to their energy at 2.8 K, state (1) being the ground state at that temperature.

The two-level, three-level, and combined relaxation models as described in the theory section were used to fit the Mössbauer spectra of $NH_4Co_{0.994}Fe_{0.006}Cl_3$ below T_{N_1}. B was fixed to the value of 22.3 T for all the fits. In fits using the three-level and combined relaxation models the energy of state (3) was fixed to the values calculated from the electronic Hamiltonian.

No significant improvement in goodness of fit was observed in fits using the more sophisticated relaxation models. This was expected since the two-level relaxation model has enough parameters to enable the spectra to be fitted well.

The energy of state (1) relative to state (2) is plotted in figure 4. At temperatures below 10 K fits using the two-level, three-level, and combined relaxation models yield the same E_2 parameter as expected given the low occupation probability of state (3) calculated from the eigenvalues of the electronic Hamiltonian. For the two-level relaxation model, the departure of E_2 from the calculated curve at temperatures above 17.5 K is consistent with state (3) becoming more populated, causing a breakdown of the two-level relaxation model. For E_2 obtained from the three-level and combined relaxation models, the deviation from the calculated curve above 22.5 K can be attributed to fixing state (3) to too low an energy. It is likely that state (3) has a higher energy than that calculated since one-dimensional correlations (causing splitting of the magnetic states) are present above T_{N_1}, whereas the calculation assumes that magnetic exchange splitting occurs only at temperatures below T_{N_1}.

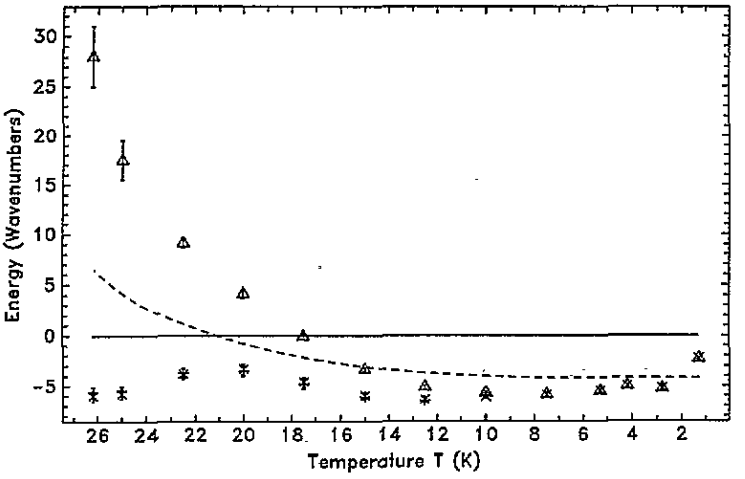

Figure 4. Electronic energy levels of Fe^{2+} in $NH_4Co_{0.994}Fe_{0.006}Cl_3$. The energy of state (1) relative to state (2) (the line at zero energy). The parameter E_2, which is the energy of state (2) minus the energy of state (1), is given by the negative of the energy scale. The dashed curve is calculated from equation (2), the Δ are from fits using the two-level relaxation model, the $\times$ are from fits using the three-level model, and the + are from fits using combined relaxation.

The electronic relaxation parameter ω_0 was found to vary by a factor of three for fits in the temperature range 2.8 to 25 K. This variation may be considered small in the context of the electronic relaxation rates obtained from fits using the two-level relaxation model, which increase by a factor of approximately 50 over the temperature range from 2.8 to 15 K.

A consistent set of soliton relaxation rate and B_{hf} parameters could be obtained using any of the two-level, three-level, or combined relaxation models if the spectra taken below 10 K were fitted with electronic relaxation only, while the spectra taken above 12.5 K were fitted with two subspectra, the soliton relaxation subspectrum with relative area of $\frac{1}{3}$, and the electronic relaxation subspectrum with a relative area of $\frac{2}{3}$. Consistent parameter sets could not be obtained if the soliton relaxation subspectrum was omitted above 12.5 K, or if a soliton relaxation subspectrum was included at temperatures below 10 K. On this basis T_{N_2} may be given as (11 ± 2) K.

The soliton relaxation rates obtained from fitting $NH_4Co_{0.994}Fe_{0.006}Cl_3$ Mössbauer

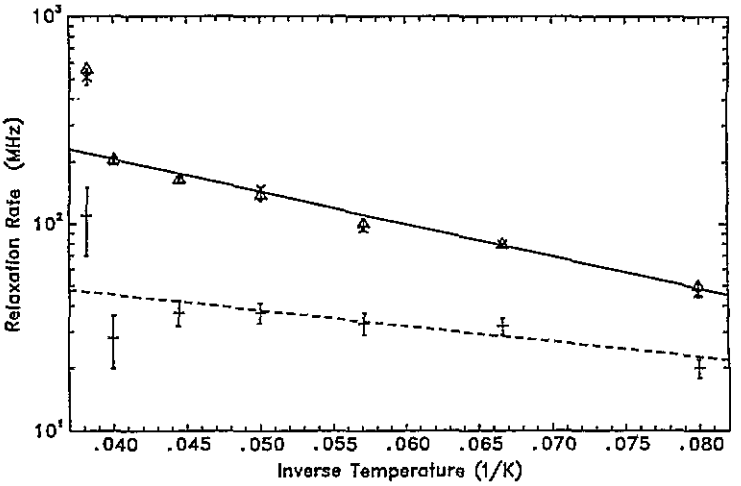

Figure 5. The soliton relaxation rates obtained from fits to Mössbauer spectra of $NH_4Co_{0.994}Fe_{0.006}Cl_3$ using the two-level (Δ), three-level (×), and combined (+) relaxation models. The solid (dashed) line is a line of best fit to the relaxation rates obtained from the two-level and three-level relaxation models (combined relaxation model).

spectra using the two-level, three-level, and combined relaxation models are plotted in figure 5. The soliton relaxation rates obtained from fits using the two-level and three-level relaxation models were the same within uncertainty, so the only effect of adding the third electronic state to the two-level relaxation model was to change the fitted energy splitting between states (1) and (2). Due to the effect of including electronic relaxation in the soliton relaxation subspectrum, the soliton relaxation rate fitted using the combined relaxation model is slower than that using the two-level and three-level relaxation models. The equation of the line of best fit to the soliton relaxation rate determined from fits using the two-level and three-level relaxation models to the Mössbauer spectra of $NH_4Co_{0.994}Fe_{0.006}Cl_3$ (the solid line in figure 5) is

$$R = (880 \pm 200) \exp\left(\frac{-(36 \pm 4)}{T}\right)$$

where the soliton relaxation rate R is in MHz, and the temperature T is in K. The dashed line in figure 5 is a line of best fit for the soliton relaxation rate as determined by fits using the combined relaxation model. It has the equation

$$R = (90 \pm 30) \exp\left(\frac{-(17 \pm 7)}{T}\right).$$

4.3. Mössbauer spectra of $CsCo_{0.99}Fe_{0.01}Cl_3$

Mössbauer spectra of a powder sample of $CsCo_{0.99}Fe_{0.01}Cl_3$ have been previously recorded in a study in this laboratory (Ward *et al* 1987). The Mössbauer spectra taken above T_{N_1} consist of a quadrupole split pair of absorption lines, similar to those of $NH_4Co_{0.994}Fe_{0.006}Cl_3$ in its paramagnetic phase. The electronic Hamiltonian parameters of Fe^{2+} in $CsCo_{0.99}Fe_{0.01}Cl_3$ and the empirical correction factor for the line intensities for the preferentially oriented powder absorber were obtained as in Ward *et al* (1987). The energy level structure and B_{hf} produced by the eigenstates was similar to those found for $NH_4Co_{0.994}Fe_{0.006}Cl_3$, with B for $CsCo_{0.99}Fe_{0.01}Cl_3$ being 24.8 T. Using these results, the

Mössbauer spectra taken at temperatures below T_{N_1} were fitted using the two-level, three-level, and combined relaxation models.

Again, as found for $NH_4Co_{0.994}Fe_{0.006}Cl_3$, no significant improvement in goodness of fit was observed in fits using the more sophisticated relaxation models.

The energy of state (1) relative to state (2) is plotted in figure 6. At temperatures above 14 K the fitted energy of state (1) obtained using the two-level relaxation model is higher than that obtained from the three-level and combined relaxation models, consistent with state (3) being occupied at these temperatures. The uncertainty of the energy splitting E_2 at 20.1 K is very large, due to the lack of structure of the Mössbauer spectrum. The large value of E_2 at this temperature may not be significant.

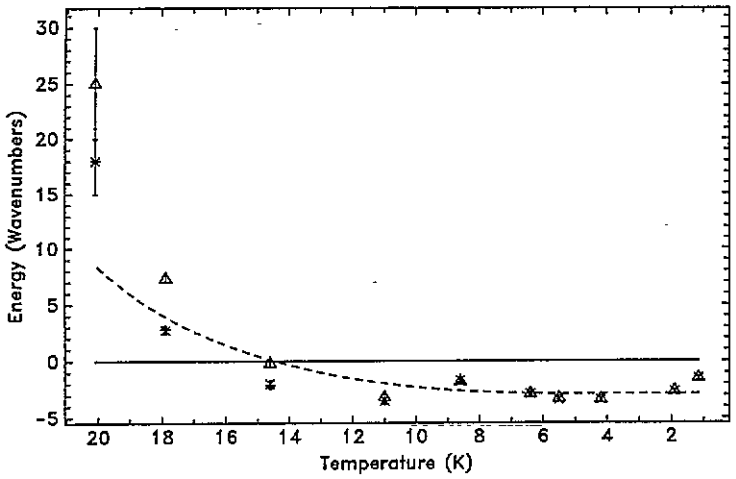

Figure 6. Electronic energy levels of Fe^{2+} in $CsCo_{0.99}Fe_{0.01}Cl_3$. The energy of state (1) relative to state (2) (the line at zero energy). The parameter E_2, which is the energy of state (2) minus the energy of state (1), is given by the negative of the energy scale. The dashed curve is calculated from equation (2), the Δ are from fits using the two-level model, the $\times$ are from fits using the three-level model, and the + are from fits using combined relaxation.

The electronic relaxation parameter ω_0 varied by a factor of five between 1.9 and 17.9 K. The larger variation in values of ω_0 determined from the Mössbauer spectra of $CsCo_{0.99}Fe_{0.01}Cl_3$ compared to those determined from $NH_4Co_{0.994}Fe_{0.006}Cl_3$ may be caused by the poorer signal to noise ratio for some of the $CsCo_{0.99}Fe_{0.01}Cl_3$ spectra.

For $CsCo_{0.99}Fe_{0.01}Cl_3$ at temperatures below 8.6 K the Mössbauer spectra could be fitted with or without a soliton subspectrum. Above this temperature it was necessary to include a soliton relaxation subspectrum in order to fit the spectra. The soliton relaxation rates obtained from fits for the various models are shown in figure 7. The solid line is a line of best fit to the soliton relaxation rates determined from fits to the Mössbauer spectra of $CsCo_{0.99}Fe_{0.01}Cl_3$ using the two-level and three-level relaxation models, and is given by the equation

$$R = (2.3 \pm 0.6) \times 10^4 \exp\left(\frac{-(70 \pm 20)}{T}\right)$$

where the soliton relaxation rate R is in MHz, and the temperature T is in K.

The dashed line is a line of best fit to the soliton relaxation rate obtained from fits using

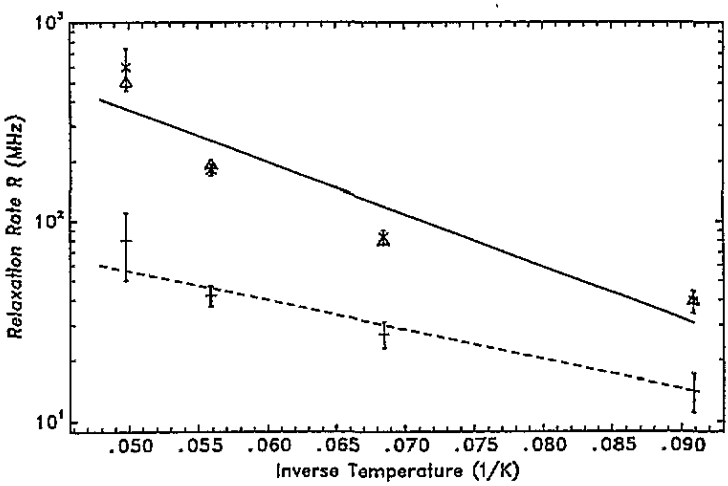

Figure 7. The soliton relaxation rates obtained from fits using the two-level (△), three-level (×), and combined (+) relaxation models. The solid (dashed) line is a line of best fit to the soliton relaxation rates obtained using the two-level and three-level relaxation models (combined relaxation model).

the combined relaxation model. Its equation is

$$R = (300 \pm 100) \exp\left(\frac{-(34 \pm 8)}{T}\right).$$

5. Discussion of results

The soliton relaxation rate R can be calculated from the theory for an ideal soliton gas in an Ising-like chain (Smit *et al* 1989) as the product of the soliton density and the thermally averaged soliton velocity,

$$R(T) = \frac{8k}{h} T \sinh\left(\frac{2\varepsilon J}{kT}\right) \exp\left(\frac{-J}{kT}\right). \tag{18}$$

Using the intrachain exchange parameters $J = 75$ K and $\varepsilon = 0.12$, R is calculated to be in the range 10^4–10^5 MHz over temperatures from 12 to 20 K.

The soliton relaxation rates obtained from fits to the Mössbauer spectra of $NH_4Co_{0.994}Fe_{0.006}Cl_3$ were slightly slower than those obtained from $CsCo_{0.99}Fe_{0.01}Cl_3$. The intrachain exchange parameters for NH_4CoCl_3 are expected to be similar to those for $CsCoCl_3$, so the predicted ideal soliton gas relaxation rates are similar though no other data for NH_4CoCl_3 have been found in the literature.

The soliton relaxation rates in $CsCoCl_3$ obtained from neutron inelastic scattering (Boucher *et al* 1985), ^{133}Cs nuclear magnetic resonance (Adachi *et al* 1979), and μ^+ spin resonance (Mekata 1990) fall in the range 10^3 to 2×10^4 MHz at 20 K. These results lie between the relaxation rates found in this experiment (80 to 600 MHz at 20 K) and the predictions of the ideal soliton gas theory (8×10^4 MHz at 20 K). A comparison of these relaxation rates provides evidence that the ideal soliton gas predicts a soliton relaxation rate which is too high. The relaxation rate obtained from the Mössbauer spectra of $CsCo_{0.99}Fe_{0.01}Cl_3$ is lower than for pure $CsCoCl_3$ found using the other experimental techniques. This may be due to the presence of the iron changing the soliton dynamics.

Also there are some problems in determining the part of the spectrum due to electronic relaxation, in particular the assumption that in the relaxation rate the parameter ω_0 in equation (12) is independent of the states involved in the relaxation process. Despite these problems, the most satisfactory relaxation model is the combined relaxation model, since it does not need to assume that soliton and electronic relaxation occur at very different rates and it includes all occupied electronic levels in the analysis.

NH_4CoCl_3 was demonstrated to have similar magnetic properties to $CsCoCl_3$, with solitons existing in the partially disordered phase, and $T_{N_2} = (11 \pm 2)$ K.

Acknowledgments

This work was supported by a University of Canterbury research grant. We gratefully acknowledge the assistance of Dr Q A Pankhurst who recorded the 2.8 K and 1.3 K Mössbauer spectra.

References

Abragam A 1961 *The Principles of Nuclear Magnetism* (London: Oxford University Press) p 447
Abragam A and Bleaney B 1970 *Electron Paramagnetic Resonance of Transition Ions* (Oxford: Clarendon)
Achiwa N 1969 *J. Phys. Soc. Japan* **27** 561
Adachi K 1981 *J. Phys. Soc. Japan* **50** 3904
Adachi K, Hamashima M, Ajiro Y and Mekata M 1979 *J. Phys. Soc. Japan* **47** 780
Asch L, Friedt J M, Lupiani C and Tornero J 1973 *Chem. Phys. Lett.* **21** 595
Ballhausen C J 1962 *Introduction to Ligand Field Theory.* (New York: McGraw-Hill) p 103
Blume M and Tjon J A 1968 *Phys. Rev.* **165** 446
Boucher J P, Regnault L P, Rossat-Mignod J, Henry Y, Brouillot J and Stirling W G 1985 *Phys. Rev.* B **31** 3015
Euler W B and Garrett B B 1981 *J. Phys. Chem. Solids* **42** 7
Ingalls R L 1971 *An Introduction to Mössbauer Spectrocopy* ed L May (New York: Plenum) p 109
Kittel C 1976 *Introduction to Solid State Physics* (New York: Wiley) p 438
Mekata M 1990 *J. Magn. Magn. Mater.* **90 & 91** 247
Mekata M and Adachi K 1978 *J. Phys. Soc. Japan* **44** 806
Melamud M, Pinto H, Makovsky J and Shaked H 1974 *Phys. Status Solidi* b **63** 699
Nagler S E, Buyers W J L, Armstrong R L and Briat B 1983 *Phys. Rev.* B **27** 1784
Ohta H, Imagawa S, Motokawa M and Ikeda H 1993 *J. Phys. Soc. Japan* **62** 2481
Sheen N I, McCann V H and Pankhurst Q A 1994 *Hyperfine Interact.* **93** 1547
Shiba H 1980 *Prog. Theor. Phys.* **64** 466
Smit H H A, de Groot H J M, Elmassalami M, Thiel R C and de Jongh L J 1989 *Physica* B **154** 237
Soling H 1968 *Acta Chem. Scand.* **22** 2793
Sugano S, Tanabe Y and Kamimura H 1970 *Multiplets of Transition Metal Ions in Crystals* (New York: Academic)
Swanson H E, McMurdie H F, Morris M C and Evans E H 1968 *US Natl Bur. Stand. Monograph* 25 section 6, p 5
Tellenbach U 1978 *J. Phys. C: Solid State Phys.* **11** 2287
Trees R E 1951 *Phys. Rev.* **82** 683
Villain J 1975 *Physica* **79** 1
Ward J B, McCann V H, Pankhurst Q A, Hassett W L and Price D C 1987 *J. Phys. C: Solid State Phys.* **20** 1689
Yoshizawa H and Hirakawa K 1979 *J. Phys. Soc. Japan* **46** 448
Yoshizawa H, Hirakawa K, Satija S K and Shirane G 1981 *Phys. Rev.* B **23** 2298